The weak lensing analysis of the CFHTLS and NGVS RedGOLD galaxy clusters

Carolina Parroni (carolina.parroni@obspm.fr)

Simona Mei, Thomas Erben, Ludovic Van Waerbeke, Anand Raichoor, Jes Ford, Rossella Licitra, Massimo Meneghetti, Hendrik Hildebrandt, et al.

arXiv:1705.04329

Abstract

An accurate estimation of galaxy cluster masses is essential for their use in cosmological and astrophysical studies. We studied the accuracy of the optical richness obtained by our RedGOLD cluster detection algorithm (Licitra et al. 2016ab) as a mass proxy, using weak lensing and X-ray mass measurements. We measured stacked weak lensing cluster masses for a sample of 1323 galaxy clusters in the Canada-France-Hawaii Telescope Legacy Survey W1 and the Next Generation Virgo Cluster Survey at 0.2<z<0.5, in the optical richness range 10-70. We tested different weak lensing mass models that account for miscentering, non-weak shear, the two-halo term, the contribution of the Brightest Cluster Galaxy, and the intrinsic scatter in the mass-richness relation. We calculated the coefficients of the mass-richness relation, and of the scaling relations between the lensing mass and X-ray mass proxies.

Data

Optical clusters catalogs:

- RedGOLD (CFTHLS and NGVS surveys; *Licitra et al. 2016ab*)

Shear catalogs:

- CFHTLenS W1 (*Heymans et al. 2012*, *Erben et al. 2012*)
- NGVSLenS (*Ferrarese et al. 2012*, *Raichoor et al. 2014*)

X-ray catalog:

- CFHTLS W1 XMM LSS (*Gozialiasl et al. 2014*)

Models

Non-weak shear

What we really measure is the reduced shear

$$g_t = \frac{\gamma_t}{1-k}$$

Miscentring

The offset distribution between optical and X-ray centres is approximated by a Rayleigh distribution with mode σ_{off}

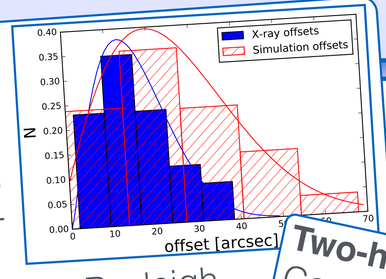

Two-halo

Contribution of the large scale structure

$$\Delta\Sigma_{tot}(R) = pcc\,[\Delta\Sigma_{NFW}(R) + \Delta\Sigma_{nl}(R)] + (1-pcc)\Delta\Sigma_{misc}(R) + \Delta\Sigma_{2halo}(R)$$

+

c-M relation (Dutton & Macciò 2014)

% of correctly centered clusters in each stack

$r_{200},\ \sigma_{off},\ pcc$	**model 1**	(base)
$\log M_{200},\ \sigma_{off},\ pcc,\ \sigma_{\ln M\|\lambda}$	**model 2**	(base + intrinsic scatter)
$r_{200},\ \sigma_{off},\ pcc,\ \log M_{BCG}$	**model 3**	(base + BCG point mass)

Analysis

We stacked clusters in five richness bins and calculated the radial shear profiles, averaging the tangential shear in logarithmic radial bins around the center of the stacked samples. We show our shear profile measurements (black), the fit results (green), the ideal profiles that we would obtain if all the clusters in the stack were perfectly centered (red) and if they were all miscentered (blue). If not taken into account, miscentering can lead to mass measurements biased low by 10-40%. We show the lensing S/N maps obtained with aperture mass statistics (*Schneider, 1996; Schirmer et al., 2006; Du & Fan, 2014*).

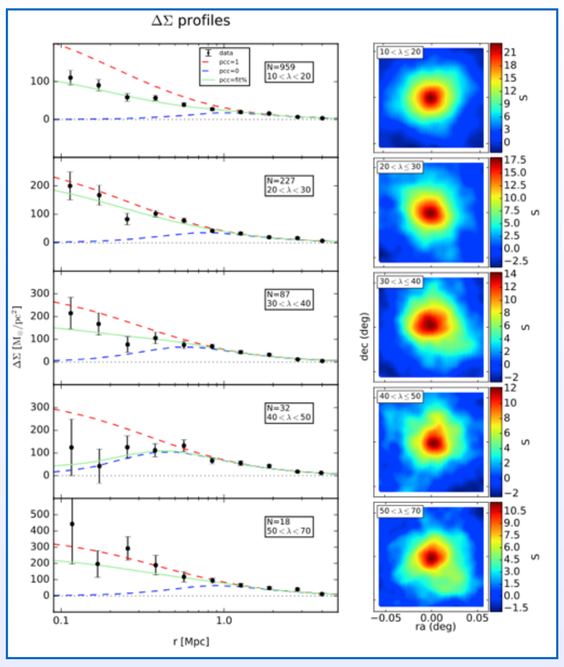

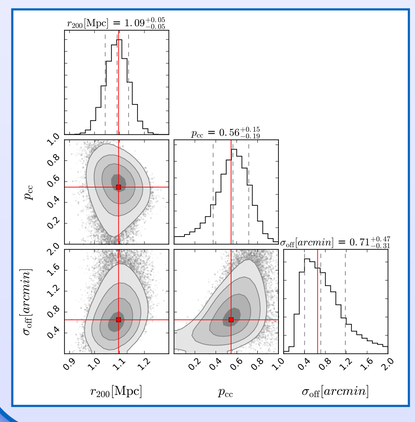

We fitted the profiles to three different models, using MCMC. On the diagonal, we show the 1-D histograms of each parameter. The 2-D histograms are also shown for each couple of parameters with confidence levels corresponding to 0.5σ, 1σ, 1.5σ, 2σ. The parameter values and errors are based on the 16th, 50th and 84th quantiles (shown as dashed lines in the 1-D histograms). The red squares and lines represents the values that correspond to the maximum likelihood.

The mass-richness relation

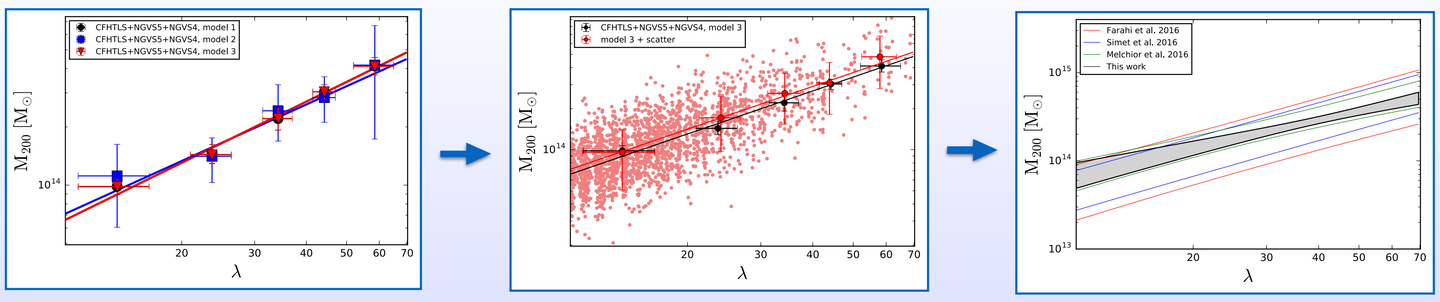

For the three models, we obtained the mass-richness relation fitting the lensing mass values recovered for each richness bin. We applied to Model 1 and 3 an *a posteriori* intrinsic scatter correction (Ford et al. 2015), which raises the normalization of the relation by ~1%. We compared our results, obtained with Model 3, with others in literature.

Lensing masses vs X-ray mass proxies

Relation	Sample	a	b	scatter
$M_L - M_X$	CC	-0.13 ± 2.96	1.02 ± 0.21	0.20
	PC	6.42 ± 3.17	0.56 ± 0.23	0.15
$M_L - M_X$	CC	0.20 ± 0.03	fixed at 1	0.20
	PC	0.23 ± 0.03	fixed at 1	0.17
$M_L - T_X$	CC	0.23 ± 0.03	1.46 ± 0.28	0.20
	PC	0.28 ± 0.03	1.03 ± 0.30	0.15
$M_L - L_X$	CC	0.10 ± 0.03	0.61 ± 0.12	0.20
	PC	0.16 ± 0.03	0.43 ± 0.12	0.15

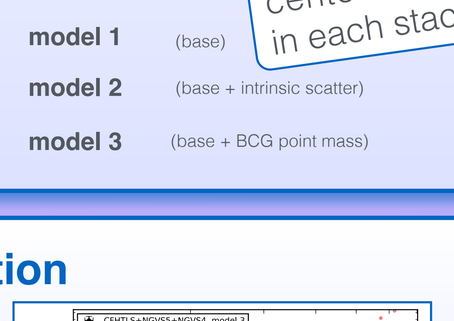

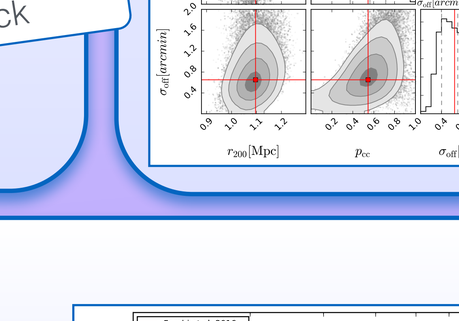

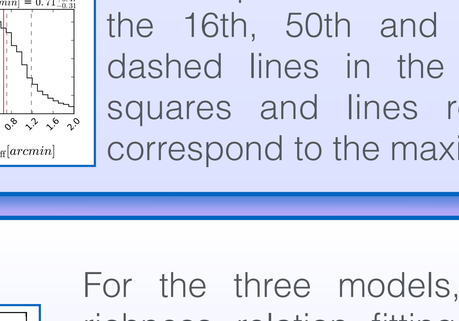

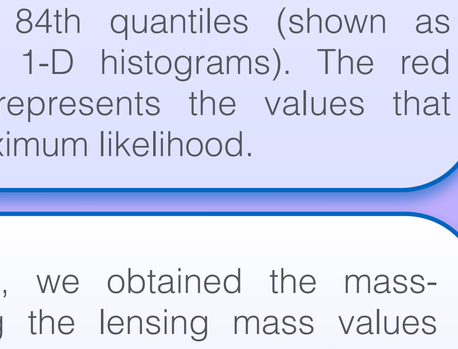

Conclusions

- We found that the intrinsic scatter in the mass-richness relation, and the BCG mass are not constrained by the data. While the miscentering correction is necessary to avoid a bias in the measured halo masses, the inclusion of the BCG mass does not affect the results.
- We calibrated RedGOLD optical richness with the lensing masses: $\log M_{200} = (14.46 \pm 0.02) + (1.04 \pm 0.09)\log(\lambda/40)$

Our results are consistent with those obtained using the SDSS and DES redMaPPer cluster samples within 1-2 σ (Rykoff et al. 2012, Saro et al. 2015, Simet et al.2016, Farahi et al. 2016, Melchior et al. 2016).

- We calculated the normalised difference and the mean ration between X-ray and lensing masses. We inferred the lensing mass vs X-ray mass, temperature, and luminosity relations. We found consistent results with other previous works in literature (Leauthaud et al. 2010, Gozaliasl et al. 2014, Kettula et al. 2015, Mantz et al. 2016).
- We found a scatter of 0.20 dex for all X-ray relations, consistent with redMaPPer scatters. This is very promising since the RedGOLD cluster sample includes lower mass values compared to redMaPPer, and the scatter does not increase as expected to these lower mass ranges.
- We found $\left\langle \frac{M_X}{M_L} \right\rangle = 0.83 \pm 0.39$. This means that weak lensing masses are on average ~20% higher than X-ray masses. This result is in agreement with both simulations and observations (Zhang et al. 2008, Meneghetti et al. 2010, Rasia et al. 2012, Simet et al. 2015).